haemagglutinin antibodies, and ectopically expressed full-length (fl) Alk (Twist-Gal4; UAS-Alk^{fl}) was immunoprecipitated with anti-Alk antibodies.

ELISA and immunofluorescence analysis

ELISA was carried out according to standard protocols. Microtitre plate wells were coated with *Drosophila* Alk monoclonal antibody 123 (ref. 1) for the sandwich ELISA, and with purified recombinant His–Jeb protein for the direct ELISA. For immunofluorescence staining, COS7 cells were transfected with either pcDNA3 (as control), pcDNA3-Alk^{fl}, pcDNA3-Alk^{E}, or pcDNA3-Alk^{A} (where superscipt E and A indicated extracellular and activated, respecitvely), and purified recombinant His–Jeb protein was added (to a final concentration of 1 $\mu g\,ml^{-1}$) for 1 h before staining, as described previously[21]. Analysis was carried out by confocal laser scanning microscopy (Leica).

In situ hybridization

In situ hybridization of whole-mount embryos was done with digoxigenin-labelled *duf* RNA as probe and followed by antibody staining as described[22].

Received 8 June; accepted 29 July 2003; doi:10.1038/nature01950.

1. Loren, C. E. *et al.* Identification and characterization of DAlk: a novel *Drosophila melanogaster* RTK which drives ERK activation *in vivo*. *Genes Cells* **6,** 531–544 (2001).
2. Loren, C. E. *et al.* A crucial role for the Anaplastic lymphoma kinase receptor tyrosine kinase in gut development in *Drosophila melanogaster*. *EMBO Rep.* **4,** 781–786 (2003).
3. Weiss, J. B., Suyama, K. L., Lee, H. H. & Scott, M. P. Jelly belly: a *Drosophila* LDL receptor repeat-containing signal required for mesoderm migration and differentiation. *Cell* **107,** 387–398 (2001).
4. Ruiz-Gomez, M., Coutts, N., Price, A., Taylor, M. V. & Bate, M. *Drosophila* dumbfounded: a myoblast attractant essential for fusion. *Cell* **102,** 189–198 (2000).
5. Strunkelnberg, M. *et al.* rst and its paralogue kirre act redundantly during embryonic muscle development in *Drosophila*. *Development* **128,** 4229–4239 (2001).
6. Fujimoto, J. *et al.* Characterization of the transforming activity of p80, a hyperphosphorylated protein in a Ki-1 lymphoma cell line with chromosomal translocation t(2;5). *Proc. Natl Acad. Sci. USA* **93,** 4181–4186 (1996).
7. Morris, S. W. *et al.* Fusion of a kinase gene, ALK, to a nucleolar protein gene, NPM, in non-Hodgkin's lymphoma. *Science* **263,** 1281–1284 (1994).
8. Falini, B. Anaplastic large cell lymphoma: pathological, molecular and clinical features. *Br. J. Haematol.* **114,** 741–760 (2001).
9. Duyster, J., Bai, R. Y. & Morris, S. W. Translocations involving anaplastic lymphoma kinase (ALK). *Oncogene* **20,** 5623–5637 (2001).
10. Morris, S. W. *et al.* ALK, the chromosome 2 gene locus altered by the t(2;5) in non-Hodgkin's lymphoma, encodes a novel neural receptor tyrosine kinase that is highly related to leukocyte tyrosine kinase (LTK). *Oncogene* **14,** 2175–2188 (1997).
11. Iwahara, T. *et al.* Molecular characterization of ALK, a receptor tyrosine kinase expressed specifically in the nervous system. *Oncogene* **14,** 439–449 (1997).
12. Klapper, R. *et al.* The formation of syncytia within the visceral musculature of the *Drosophila* midgut is dependent on duf, sns and mbc. *Mech. Dev.* **110,** 85–96 (2002).
13. Martin, B. S., Ruiz-Gomez, M., Landgraf, M. & Bate, M. A distinct set of founders and fusion-competent myoblasts make visceral muscles in the *Drosophila* embryo. *Development* **128,** 3331–3338 (2001).
14. Dworak, H. A. & Sink, H. Myoblast fusion in *Drosophila*. *Bioessays* **24,** 591–601 (2002).
15. Baylies, M. K. & Michelson, A. M. Invertebrate myogenesis: looking back to the future of muscle development. *Curr. Opin. Genet. Dev.* **11,** 431–439 (2001).
16. Bate, M. The embryonic development of larval muscles in *Drosophila*. *Development* **110,** 791–804 (1990).
17. Carmena, A., Bate, M. & Jimenez, F. Lethal of scute, a proneural gene, participates in the specification of muscle progenitors during *Drosophila* embryogenesis. *Genes Dev.* **9,** 2373–2383 (1995).
18. Gabay, L., Seger, R. & Shilo, B. Z. MAP kinase in situ activation atlas during *Drosophila* embryogenesis. *Development* **124,** 3535–3541 (1997).
19. Patel, N. H. Imaging neuronal subsets and other cell types in whole-mount *Drosophila* embryos and larvae using antibody probes. *Methods Cell Biol.* **44,** 445–487 (1994).
20. Campos-Ortega, J. A. & Hartenstein, V. The Embryonic Development of Drosophila Melanogaster. (Springer, Berlin, 1997).
21. Palmer, R. H. *et al.* DFak56 is a novel *Drosophila melanogaster* focal adhesion kinase. *J. Biol. Chem.* **274,** 35621–35629 (1999).
22. Jiang, W. *et al.* PRC1: a human mitotic spindle-associated CDK substrate protein required for cytokinesis. *Mol. Cell* **2,** 877–885 (1998).
23. Kopczynski, C. C., Davis, G. W. & Goodman, C. S. A neural tetraspanin, encoded by late bloomer, that facilitates synapse formation. *Science* **271,** 1867–1870 (1996).

Supplementary Information accompanies the paper on **www.nature.com/nature**.

Acknowledgements The authors would like to thank T. Hunter and I. Salecker for critical reading of the manuscript, and D. Eriksson, N. Norgren and A. Sheikholvaezin for help with ELISA analysis. This work is funded by the Swedish Research Council and is also supported by The Swedish Society for Medical Research (SSMF), Åke Wibergs Fund, the Royal Swedish Academy of Sciences, Lars Hiertas Minne Fund, and the Cancer Research Fund of Northern Sweden. F.D. was supported by a post-doctoral fellowship from the Wenner-Grenska Foundation.

Competing interests statement The authors declare that they have no competing financial interests.

Correspondence and requests for materials should be addressed to R.H.P. (Ruth.Palmer@ucmp.umu.se).

Molecular identification of a danger signal that alerts the immune system to dying cells

Yan Shi[1], **James E. Evans**[2] **& Kenneth L. Rock**[1]

[1]*Department of Pathology, and* [2]*Proteomics and Mass Spectrometry Facility, Department of Biochemistry and Molecular Pharmacology, University of Massachusetts Medical School, Worcester, Massachusetts 01655, USA*

In infections, microbial components provide signals that alert the immune system to danger and promote the generation of immunity[1,2]. In the absence of such signals, there is often no immune response or tolerance may develop. This has led to the concept that the immune system responds only to antigens perceived to be associated with a dangerous situation such as infection[3,4]. Danger signals are thought to act by stimulating dendritic cells to mature so that they can present foreign antigens and stimulate T lymphocytes[2,5–7]. Dying mammalian cells have also been found to release danger signals of unknown identity[8–11]. Here we show that uric acid is a principal endogenous danger signal released from injured cells. Uric acid stimulates dendritic cell maturation and, when co-injected with antigen *in vivo*, significantly enhances the generation of responses from CD8$^+$ T cells. Eliminating uric acid *in vivo* inhibits the immune response to antigens associated with injured cells, but not to antigens presented by activated dendritic cells. Our findings provide a molecular link between cell injury and immunity and have important implications for vaccines, autoimmunity and inflammation.

When dying cells are co-injected with antigen into animals, they provide an adjuvant effect for priming T-cell responses[10,11]. This endogenous adjuvant activity is present in the cytosol of cells and markedly increases when cells are injured, for example, by ultraviolet irradiation. To identify this endogenous adjuvant, here we fractionated cytosol from ultraviolet-irradiated BALB/c 3T3 cells by high-performance liquid chromatography (HPLC) on a sizing column monitored with a diode array ultraviolet spectrum detector (Fig. 1a). Pools of 4–5 consecutive fractions were tested for their ability to augment the priming of CD8$^+$ T-cell responses when co-injected with particulate HIV gp120 antigen. After 14 d, splenocytes from the primed mice were stimulated *ex vivo* with antigen and then assayed for their ability to kill antigen-bearing target cells in a ^{51}Cr-release assay[10].

A pool of low molecular weight (LMW) fractions that were below the optimal resolution range (relative molecular mass less than 5,000; $M_r < 5K$) of the sizing columns had adjuvant activity that markedly enhanced the generation of cytotoxic T lymphocyte (CTL) responses (Fig. 1b). When the individual components of this active LMW pool were tested, most of the activity was located in a single fraction (Fig. 1b, inset). Another pool of higher molecular weight fractions (~40–100K) also had adjuvant activity, but this has not been further studied at this time.

We focused on characterizing the LMW adjuvant. It was present in the cytosol of both ultraviolet-treated 3T3 cells and liver. LMW fractions from liver cytosol were separated further by HLPC with sequential anion exchange (Mono Q HR5/5; Fig. 1c), sizing (Superdex 200 HR 10/30; Fig. 1d) and reverse phase (C18) (Fig. 1e) columns. After each separation the active fractions were identified by their ability to boost CTL responses *in vivo* (Fig. 1f–h). On all four columns, the LMW adjuvant from liver showed the same chromatography profile as that from 3T3 cells, suggesting that both cells contained the same adjuvant molecule (data not shown). The active fractions from all four columns had unique

ultraviolet peak absorptions at 235 and 292 nm (Fig. 1a, c–e), which disappeared at low pH (data not shown).

The LMW material from the fourth HPLC column (C18) appeared to be homogeneous. It was subjected to trimethylsilylation (TMS) derivatization and analysed by gas chromatography (GC) coupled with electron impact mass spectrometry (EI-MS; Fig. 2a). A single prominent GC peak was detected at 9.88 min (Fig. 2a). The EI mass spectrum of this peak indicated a compound with an M_r of 456 containing two or more TMS groups. A search of the National Institute of Standards and Technology (NIST) database of EI mass spectra returned a very high probability match with tetra-TMS uric acid (Fig. 2b).

When this same fraction was analysed by direct infusion negative ion electrospray ionization tandem mass spectrometry (ESI-MS), an intense ion at m/z 167 was observed, consistent with the $[M\text{-}H]^-$ ion from uric acid. Isolation and subsequent collisional fragmentation of this ion produced an MS^2 product ion spectrum identical to that obtained from a uric acid standard. Similarly, MS^3 product ion spectra from the major MS^2 ion (m/z 124) matched that from uric acid (Fig. 2c–e and Supplementary Fig. 1). The pH-dependent ultraviolet absorption peaks of the LMW fraction at 235 and 292 nm matched well the expected pattern for the enol tautomer of uric acid (Fig. 2f). To exclude the possibility of an enantiomeric or stereo-isomeric structure, the purified LMW molecule was incubated with uricase, a highly specific enzyme that breaks down uric acid to allantoin. Uricase rapidly destroyed the LMW molecule (Fig. 2g). Together, these data show that the main constituent of the highly purified LMW fraction is uric acid.

To evaluate further whether uric acid was responsible for the biological activity seen *in vivo*, we purchased highly purified uric acid and tested it for adjuvant activity. This material enhanced CTL priming to a similar extent to that achieved by the purified LMW fraction (Fig. 3a, b). Comparable results were obtained when C57BL/6 mice were immunized with pure uric acid and particulate ovalbumin antigen (Supplementary Fig. 2). Treatment of the LMW fraction with uricase significantly reduced its adjuvant activity, providing further proof that uric acid was the active component in this fraction (Fig. 3d, e). Both the purified LMW fraction and the commercial uric acid had adjuvant activity in lipopolysaccharide (LPS)-nonresponsive mice lacking the Toll-like receptor 4 (TLR4; Fig. 3g, h). Thus, LPS is not responsible for the adjuvant activity in our preparations. The finding that uricase inactivated the LMW fraction also argues that LPS or other microbial contaminants do not account for the adjuvant activity (Fig. 3). Because both commercially obtained uric acid and uric acid purified to homogeneity from liver have adjuvant activity and uricase destroys this activity, we conclude that uric acid is one of the endogenous adjuvants in cells.

We have previously reported that endogenous adjuvant activity markedly increases in cells when they are injured in ways that cause them to undergo apoptosis[10]. Consistent with this observation, we found that uric acid in EL4 cells increased markedly after treatment with heat shock, cycloheximide and emetine (Fig. 3j), which we have previously shown to increase adjuvant activity. We also observed about a fourfold increase in uric acid when 3T3 cells were treated with ultraviolet radiation (Fig. 3j).

These findings provide insight into the mechanism underlying the increase in endogenous adjuvant in injured cells. Uric acid is produced during the catabolism of purines and is the end product of this process in uricotelic mammals. Thus, as the injured cells rapidly degrade their RNA and DNA, the liberated purines will be converted into uric acid, leading to its accumulation. The production of uric acid does not require protein synthesis, which enables dying cells to produce more danger signal and explains why this increase is not blocked by protein synthesis inhibitors[10].

The amount of uric acid needed to provide an adjuvant effect when injected *in vivo* was about 10 μg in 100 μl (Fig. 3k). The active fractions from HPLC purification that were injected into mice all contained more than this amount of uric acid (>170 μg ml^{-1}). Ten micrograms of uric acid was produced by about 3×10^6 3T3 cells

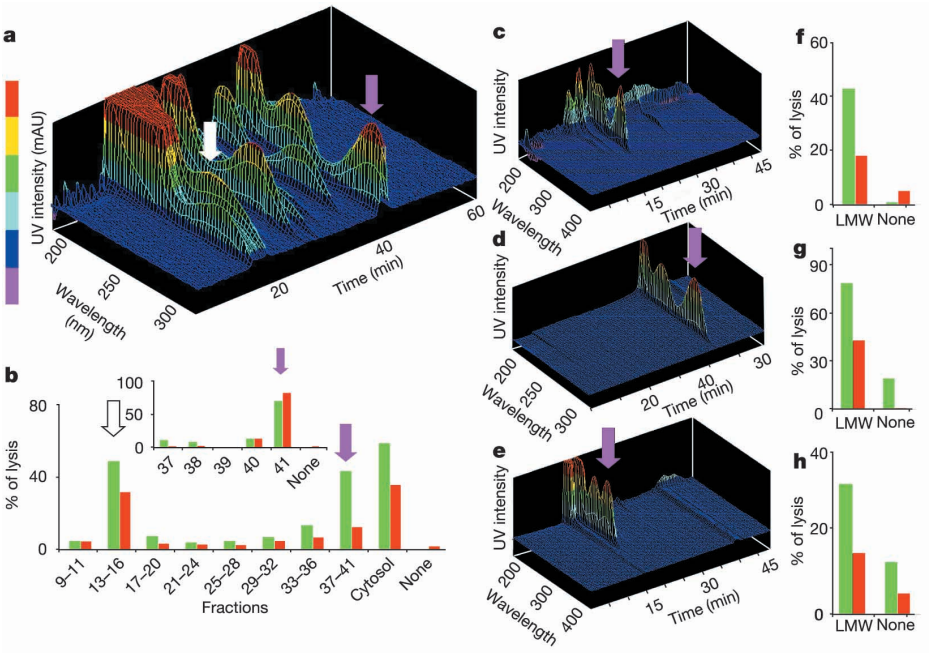

Figure 1 Purification of the LMW endogenous adjuvant from cytosol. **a**, Ultraviolet spectrum of 3T3 cytosolic fractions from a GF250 sizing column. **b**, Anti-HIV-gp120 specific CTL activity from BALB/c mice injected with HIV gp120 antigen beads alone (none), or admixed with either unfractionated cytosol or pooled fractions from **a**. Green and red bars indicate the percentage of specific lysis at effector : target ratios of 100:1 and 33:1, respectively. Inset, individual analysis of LMW fractions 37–41. **c**–**e**, Ultraviolet spectra of the sequential purification of LMW fractions on anion exchange (**c**), sizing (**d**) and reverse phase (**e**) columns. **f**–**h**, CTL activity from mice injected with HIV gp120 and the active LMW fractions from **c**–**e**, respectively. In **a**–**e**, the active LMW and HMW fractions are indicated by pink and white arrows, respectively.

treated with ultraviolet radiation (Fig. 3). Such numbers of cells could easily die in tumours, and during viral infections and other pathological situations. In fact, it is well known that large amounts of uric acid can be produced from tissue injury *in vivo*[12].

If uric acid is a physiologically important danger signal that promotes immunity, then its elimination *in vivo* should result in reduced T-cell responses to antigen. To test this hypothesis, 3T3 cells were treated with allopurinol (a uric acid analogue that reduces uric acid production) and then injured by ultraviolet irradiation and freezing. These cells were then injected, along with gp120 beads, into mice treated with allopurinol and uricase (to destroy any uric acid that was released *in vivo*). Allopurinol and uricase treatment of mice markedly reduced plasma uric acid concentrations (Supplementary Fig. 3). The priming of gp120-specific CTLs by 10^4 injured cells was substantially reduced by eliminating uric acid (Fig. 4a). Cultures of CTLs from control mice contained 11.8 lytic units as compared with 2.0 lytic units in CTLs from mice treated with allopurinol plus uricase (83% inhibition, Fig. 4b; representative of several experiments). CTLs were still generated in treated mice that were injected with larger numbers of injured cells (10^5). This may be due to the presence of other endogenous adjuvants or the incomplete elimination of uric acid. In the mice treated with allopurinol plus uricase, however, 10^5 injured 3T3 cells stimulated an anti-gp120-specific CTL response equivalent to that induced by 10^4 injured 3T3 cells in control mice (Fig. 4a). In other words, elimination of uric acid reduced the priming of CTLs by about 90%.

To exclude the possibility that the allopurinol and uricase treatment was nonspecifically immunosuppressive, we immunized both treated and control mice with activated bone-marrow-derived dendritic cells that were pulsed with a synthetic peptide corresponding to the gp120 epitope. As expected, the peptide-pulsed dendritic cells primed CTL responses without any added adjuvant (Fig. 4c). Notably, the generation of anti-gp120 CTLs was not reduced in the treated mice even under limiting conditions (Fig. 4c). The increased response seen in the treated mice was not observed in other experiments. Therefore, the elimination of uric acid *in vivo* selectively reduces T-cell responses that are stimulated by injured cells. We conclude that uric acid is one of the chief mediators produced by injured cells that signals danger and promotes immune responses.

Adjuvants are thought to work, at least in part, by stimulating dendritic cells to mature and to increase their expression of costimulatory molecules[1,5,6]. We found that when uric acid was added to cultures of primary bone-marrow-derived dendritic cells (>95% $CD11C^+$), it stimulated them to increase rapidly (within 6 h) their expression of CD86 and, to a lesser extent, CD80 (Fig. 5a). This stimulation was stronger than that produced by LPS (Fig. 5b). This effect was also seen with dendritic cells from TLR4-null mice and therefore was not due to contaminating LPS (Fig. 5b). Although uric acid stimulated dendritic cells to increase their expression of costimulatory molecules, it did not affect their rate of phagocytosis of antigen particles (Supplementary Fig. 4).

We noted that the concentrations of uric acid that stimulated dendritic cells were also those in which crystals precipitated (Fig. 5c and Supplementary Fig. 5). We also found that preformed monosodium urate (MSU) crystals were highly stimulatory, whereas soluble uric acid was not (Fig. 5b). It is therefore likely that MSU crystals are the biologically active form *in vitro*. It is also possible that crystals are the active form *in vivo*, because uric acid is reported

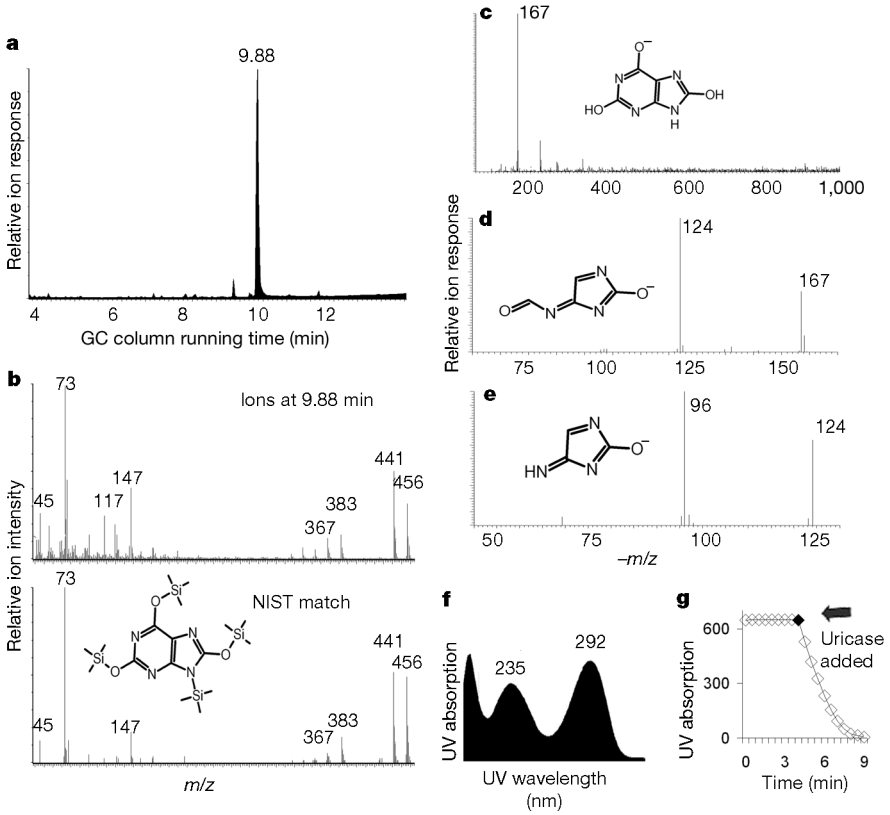

Figure 2 Molecular identification of the LMW endogenous adjuvant. **a**, Total ion current plot from GC-EI-MS analysis of a TMS-derivatized LMW active fraction purified as in Fig. 1e. **b**, Top, full EI-MS of the 9.88-min fraction in **a**. Bottom, matching mass spectrum from the NIST database and the structure of tetra-TMS uric acid (inset). **c**, Infusion negative ion ESI-MS spectrum of the same fraction. **d**, **e**, MS^2 and MS^3 product ion spectra of the *m/z* 167 and *m/z* 124 ions from **c** and **d**, respectively. Insets, proposed product ion structures. Uric acid yielded the identical initial ion and subsequent fragments (Supplementary Fig. 1). **f**, Ultraviolet spectrum of a uric acid standard at neutral pH. **g**, Uricase degradation of the highly purified LMW fraction assayed by the reduction of ultraviolet absorption at 292 nm.

to be saturating and to precipitate *in vivo* at the concentrations that we injected (>70 μg ml^{-1})[13]. Although the concentration of uric acid varied from 170 to 1,600 μg ml^{-1} in our active HPLC fractions, it remained in solution because it is more soluble in buffers than in body fluids (refs 14–18 and Fig. 1). In addition, the concentration of uric acid in our preparations of liver cytosol is typically about 4 mg ml^{-1}, which when released *in vivo* should locally produce a highly supersaturated condition. Preformed MSU crystals also had adjuvant activity when injected *in vivo* (Fig. 5d). Thus, these data suggest that a chemical phase transition could be the key event that transforms a normal autologous component into a danger signal.

We next investigated whether any crystalline or particulate material would stimulate dendritic cells. Particles of aluminium hydroxide (alum, a weak adjuvant for antibody responses; Fig. 6a) or polystyrene (data not shown) did not stimulate dendritic cells *in vitro* to increase expression of CD86. In marked contrast to MSU crystals (Figs 6a and 5a–c), crystals of allopurinol, a molecule that is structurally very similar to uric acid, or of basic calcium phosphate (BCP) failed to activate dendritic cells (Fig. 6a). Similarly, the co-injection of BCP crystals, allopurinol crystals or alum *in vivo* all failed to augment T-cell responses to gp120, whereas MSU crystals provided a strong adjuvant effect (Fig. 6b). These results show that MSU crystals have specific ability to activate dendritic cells and to augment the priming of T cells; therefore, these biological effects are unlikely to be due to a simple mechanical stimulation of dendritic cells by particles.

In hyperuricemia, MSU crystals can precipitate in joints, where they cause gout, and/or in other tissues causing inflammation[13,19]. In these situations, the crystals stimulate monocytes, macrophages and epithelial cells to produce inflammatory mediators[20–22]. It seems likely that dendritic cells are stimulated in a similar fashion and that the activation of several of these cells of the innate immune system contributes to the adjuvant effect of uric acid. Our findings also raise the possibility that dendritic cells are involved in the pathogenesis of gouty inflammation.

Our findings have several possible implications for health and disease. Up until now, MSU crystals were viewed solely as pathogenic and the biological response to them as pathological. Our findings suggest that the formation of these crystals and the ensuing host response could have an important role in immune surveillance and the generation of adaptive immunity. In addition, it is well known that *in vivo* dying tissue initially provokes a strong inflammatory response but loses this phlogistic quality as it is depleted of its unidentified proinflammatory mediators[23]. Our data raise the possibility that uric acid is one of the mediators that leads to the inflammatory response to injured and dying tissues. Thus MSU might also be involved in inflammation to injury.

In terms of immune surveillance, our data suggest a model in which dying cells release uric acid together with their antigens. Dendritic cells ingest the cellular debris and thereby acquire antigens from the dying cells. At the same time they receive a 'danger signal' from the uric acid (and maybe other endogenous adjuvants) and are stimulated to mature and to become immunostimulatory. Thus, uric acid alerts the immune system to cell death, which is a

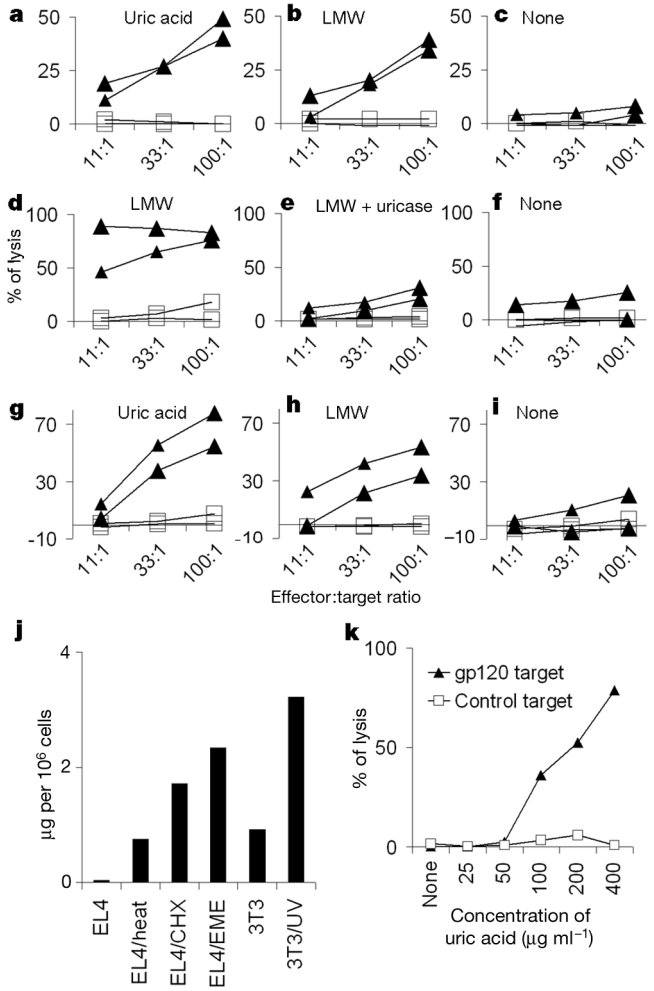

Figure 3 Uric acid has adjuvant activity *in vivo* and its concentrations increase in injured cells. **a**–**c**, CTLs from BALB/c mice immunized with uric acid (50 μg) (**a**), the LMW fraction (purified as in Fig. 1e) (**b**) or PBS (**c**) mixed with 5 μg of gp120–latex beads were assayed on gp120^{+} (filled triangles) or control (open squares) targets; data points represent individual mice. **d**–**f**, As **a**–**c**, except that untreated (**d**) or uricase-treated (**e**) LMW fractions were injected. **g**–**i**, As **a**–**c**, except that C.C3H/lps-d (*Tlr4*$^{-/-}$) mice were used. **j**, Uric acid content in EL4 or 3T3 cells after no treatment, or treatment with heat shock (heat), cycloheximine (CHX), emetine (EME) or ultraviolet irradiation (UV). **k**, As **a**, except that the amount of uric acid co-injected was varied. Values are the mean lysis at an effector:target ratio of 100:1 for two mice.

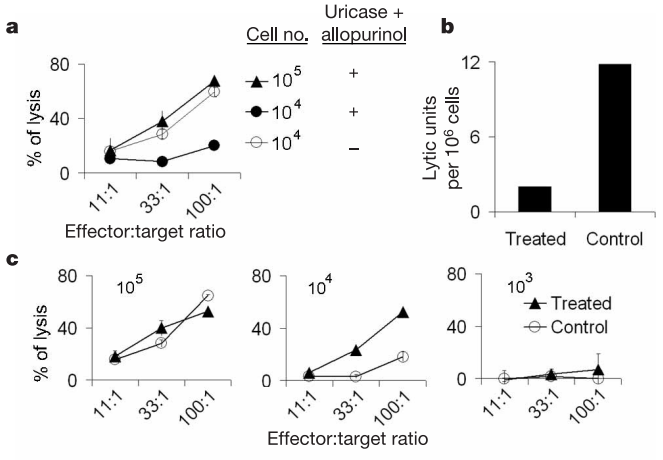

Figure 4 Eliminating uric acid *in vivo* inhibits adjuvant activity from injured cells. **a**, Mice treated with uricase and allopurinol were immunized with 10^4 (filled circles) or 10^5 (filled triangles) injured 3T3 cells (Methods) treated with uricase and allopurinol plus gp120–latex beads (2 μg), and assayed as in Fig. 1b. Control mice (open circles) were assayed similarly except that uricase and allopurinol were omitted from all steps. Data are the mean ± range of lysis for two mice. **b**, Analysis of lytic units from the cells in **a** (treated versus untreated mice receiving 10^4 cells). **c**, 10^5 (left), 10^4 (middle) or 10^3 (right) gp120 peptide-pulsed dendritic cells were injected s.c. into mice that had been treated with (filled triangles) or without (open circles) uricase and allopurinol, and assayed as in Fig. 1b (Methods).

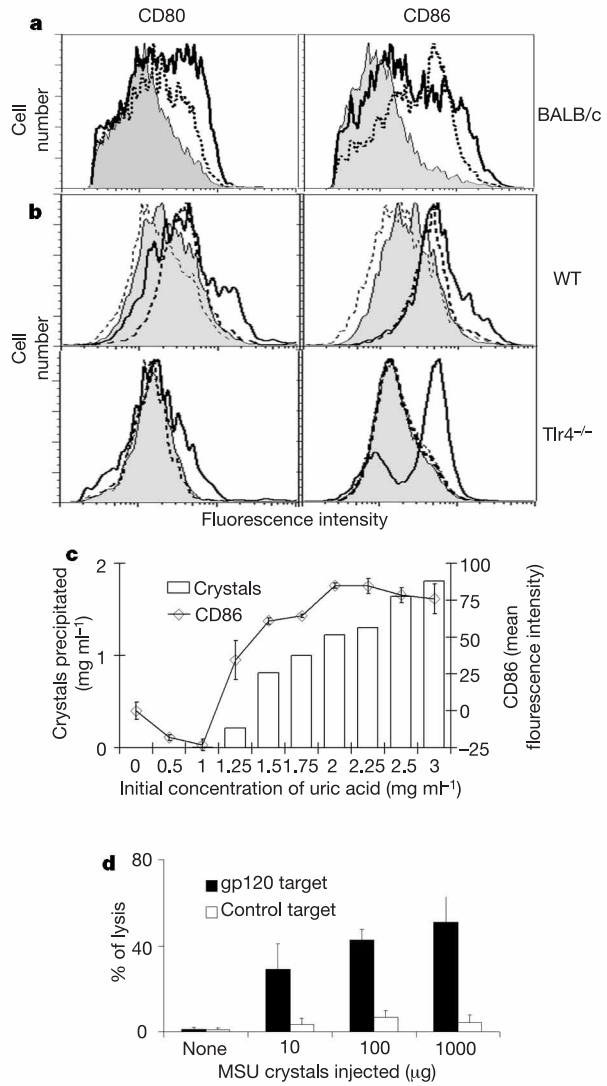

Figure 5 MSU crystals rapidly activate dendritic cells. **a**, Expression of CD80 and CD86 on BALB/c bone-marrow-derived dendritic cells that were either untreated (shaded area) or incubated with 20 μl of MSU crystals for 6 h (broken lines) or 24 h (unbroken lines). **b**, As **a**, except that dendritic cells from wild-type C57BL/6 (WT) or C.C3H/lps-d (*Tlr4*$^{-/-}$) mice were untreated (shaded areas), incubated with soluble uric acid (70 μg ml^{-1}, thin broken lines), 1 μg ml^{-1} LPS (thick broken lines) or 20 μl of MSU crystals per well (thick unbroken lines) for 6 h. **c**, Expression of CD86 on dendritic cells (diamonds) versus the quantity of MSU crystals forming in cultures (bars) incubated for 24 h with the indicated concentrations of uric acid. **d**, As Fig. 3a, except that preformed MSU crystals were injected into mice, and data are the mean ± range of lysis at an effector : target ratio of 100:1 of gp120-transfected (filled bars) or control transfected (open bars) targets for two mice.

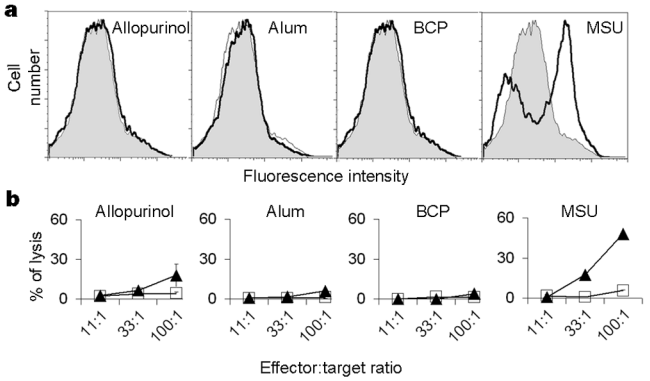

Figure 6 Specificity of dendritic cell activation by MSU crystals. **a**, As Fig. 5a except that BALB/c bone-marrow-derived dendritic cells were incubated for 6 h in 2 ml of media containing 0.5 mg ml^{-1} of crystals of allopurinol, BCP or MSU, or alum (Methods). Unbroken line indicates CD86 expression, the shaded curve indicates background (untreated dendritic cells). **b**, BALB/c mice were immunized with 500 μg of the indicated crystals or alum admixed with gp120–latex beads (2 μg) and assayed as in Fig. 5d. Values are the mean ± range of lysis of targets by CTLs from two mice.

hallmark of potential danger to the host. If the dying cell contains antigens to which the host is not tolerant, then an immune response will be stimulated. This therefore provides a mechanism by which the immune system could generate responses against tumours and viral infections that were thought to lack adjuvants.

Our *in vitro* data indicate that the immunostimulatory form of uric acid may be MSU crystals. Uric acid is relatively insoluble in biological fluids (70 μg ml^{-1}) and mammals have relatively high constitutive concentrations of uric acid in the blood (40–60 μg ml^{-1}). Because cytosol contains high concentrations of uric acid (for example, 4 mg ml^{-1}, which increases even more when injured cells degrade their RNA and DNA), the local environment around the dying cells should become supersaturated with uric acid released when cell lyse. This would favour the formation of MSU. The MSU crystals would also stimulate monocytes and epithelial cells to produce cytokines, which may further potentiate immune responses[13]. In the same way, the danger signal provided by uric acid and other endogenous adjuvants might underlie the initiation of autoimmunity in genetically susceptible individuals. In this context, individuals affected with some autoimmune diseases have been reported to have a higher incidence of hyperuricaemia than controls[19,24].

There also remains a need for the development of more and better adjuvants for use in humans. Alum, the only adjuvant approved for human use, is relatively weak, does not generally elicit CD8 immunity, and may preferentially induce responses biased toward T-helper type 2 cells[1]. Uric acid represents a previously unknown class of adjuvant that is distinct from those of microbial origin. It stimulates strong CD8$^+$ T-cell immunity. Our findings therefore indicate that uric acid may be useful as a type of adjuvant for vaccines.

In summary, we have identified uric acid as one of the principal endogenous immunological danger signals. It is constitutively present in cells and its concentration increases when cells are injured. When released from dying cells, it stimulates dendritic cells to mature and augments the priming of CD8$^+$ T-cell responses to cross-presented antigen. □

Methods

Mice, cells and reagents

All biochemical reagents were from Sigma. The Amplex Red kit for detecting uric acid was from Molecular Probes. MSU crystals were prepared by incubating supersaturated uric acid solutions (4–5 mg ml^{-1}) in 0.1 M borate (pH 8.5) at room temperature (26 °C) for >48 h, followed by washing with alcohol and acetone. Preparations of other crystals are described in Supplementary Information. We prepared antigen beads as described[10,25]. Peptides have been described[10] and were a gift from T. Vedvick (Corixa). Mice, cells and all other reagents have been described[10,11].

Purification and treatment of LMW adjuvant

We produced ultraviolet-treated 3T3 cells and liver cytosol as described[10]. Chromatographic separations were done with a System Gold 125 solvent module linked to a System Gold 168 diode array spectrum analyser running Gold Nouveau software v1.0 (Beckman). Cytosolic fractions were purified sequentially on Zobrax GF-250 (Agilent) or Superdex 75 HR 10/30 (Pharmacia), Mono Q HR 5/5 (Pharmacia), Superdex 200 HR 10/30 (Pharmacia) and semi-preparative C18 (Vydac) columns. HPLC procedures and buffers are described in the Supplementary Information. Where indicated, the LMW C18 fraction (containing 1/40 liver equivalent) was incubated in 500 μl of 0.1 M borate buffer (pH 8.5) at room temperature (26 °C), 0.01 unit of uricase was added, and the ultraviolet

absorption at 292 nm was monitored. In some experiments, the LMW C18 fraction (containing 1/10 liver equivalent) was treated with 0.1 units of uricase at room temperature (26 °C) before being used for injection *in vivo*.

Immunization and CTL assays

Immunizations and CTL assays were done as described[10] except that the indicated adjuvants were used. Column fractions from 1–10% liver cytosol were injected without manipulation (GF250 column) or after drying and reconstitution (other columns). Pooled fractions without adjuvant activity were usually used as negative controls. For *in vitro* stimulation, splenocytes from immunized mice were stimulated with 10^{-8} M of RGPGRAFVTI or SIINFEKL peptide directly, and assayed as described[10].

In some experiments, mice were injected with uricase (10 μg per mouse) and allopurinol (800 μg per mouse) in the peritoneum daily for 3 d, and 3T3 cells were cultured in 50 μM allopurinol. The cells were irradiated with ultraviolet as described[10], frozen for 20 min, and varying numbers were then admixed with gp120–latex beads and injected subcutaneously (s.c.) together with allopurinol (20 μg) and uricase (0.4 μg) into the pretreated mice. Alternatively, mice treated with allopurinol plus uricase were immunized s.c. with varying numbers of bone-marrow-derived dendritic cells that had been pulsed with HIV gp120 peptide RGPGRAFVTI (1 μg ml^{-1} for 1 h). Controls were treated identically except that uricase and allopurinol were omitted from all steps.

Mass spectrometry

GC-MS and ESI-MS were done with a Quattro-II triple quadrupole (Waters) and a LCQ quadrupole ion trap (Finnigan) mass spectrometer, respectively. Technical parameters, as well the method of TMS derivatization, are given in the Supplementary Information.

Uric acid measurement

EL4 cells (10^8) were resuspended in 5 ml of culture media and incubated at 37 °C for 5 h after being treated with emetine[10] or cycloheximide for 1 h or heat-shocked at 45 °C for 20 min. 3T3 cells were either untreated or exposed to ultraviolet light for 5 min and incubated for 5 h. The cells were directly suspended in culture media (without washing) and disrupted by nitrogen cavitation followed by centrifugation. We determined the concentration of uric acid in cytosol, HPLC fractions and mouse plasma by either HPLC or a uric acid kit.

Dendritic cell culture and analysis

We cultured bone-marrow-derived dendritic cells as described[26]. After removing floating cells, cultures were stimulated as indicated for 6 or 24 h. Bound crystals were detached by incubation with either 0.5% heparin or 0.5 μM polyvinyl sulphate (100K) in PBS for 10 min. The cells were then collected by scraping and extensively washed. Staining and flow cytometry have been described[11]. MSU crystals were collected from parallel sets of wells without dendritic cells, washed with absolute alcohol and dissolved in 0.1 N NaOH. The amount of uric acid was determined by measuring ultraviolet absorption at 292 nM against a set of standard uric acid and NaOH solutions.

Received 9 July; accepted 18 August 2003; doi:10.1038/nature01991.
Published online 7 September 2003.

1. Hunter, R. L. Overview of vaccine adjuvants: present and future. *Vaccine* **20** (suppl. 3), S7–S12 (2002).
2. Janeway, C. A. Jr Approaching the asymptote? Evolution and revolution in immunology. *Cold Spring Harb. Symp. Quant. Biol.* **54,** 1–13 (1989).
3. Janeway, C. A. Jr The immune system evolved to discriminate infectious nonself from noninfectious self. *Immunol. Today* **13,** 11–16 (1992).
4. Matzinger, P. Tolerance, danger, and the extended family. *Annu. Rev. Immunol.* **12,** 991–1045 (1994).
5. Cox, J. C. & Coulter, A. R. Adjuvants—a classification and review of their modes of action. *Vaccine* **15,** 248–256 (1997).
6. Schijns, V. E. Immunological concepts of vaccine adjuvant activity. *Curr. Opin. Immunol.* **12,** 456–463 (2000).
7. Medzhitov, R. & Janeway, C. Jr Innate immune recognition: mechanisms and pathways. *Immunol. Rev.* **173,** 89–97 (2000).
8. Albert, M. L., Sauter, B. & Bhardwaj, N. Dendritic cells acquire antigen from apoptotic cells and induce class I-restricted CTLs. *Nature* **392,** 86–89 (1998).
9. Gallucci, S., Lolkema, M. & Matzinger, P. Natural adjuvants: endogenous activators of dendritic cells. *Nature Med.* **5,** 1249–1255 (1999).
10. Shi, Y., Zheng, W. & Rock, K. L. Cell injury releases endogenous adjuvants that stimulate cytotoxic T cell responses. *Proc. Natl Acad. Sci. USA* **97,** 14590–14595 (2000).
11. Shi, Y. & Rock, K. L. Cell death releases endogenous adjuvants that selectively enhance immune surveillance of particulate antigens. *Eur. J. Immunol.* **32,** 155–162 (2002).
12. Jeha, S. Tumor lysis syndrome. *Semin. Hematol.* **38,** 4–8 (2001).
13. Smyth, C. J. & Holers, V. M. *Gout, Hyperuricemia, and Other Crystal-Associated Arthropathies* (Marcel Dekker, New York, 1998).
14. Kippen, I., Klinenberg, J. R., Weinberger, A. & Wilcox, W. R. Factors affecting urate solubility *in vitro*. *Ann. Rheum. Dis.* **33,** 313–317 (1974).
15. Iwata, H., Nishio, S., Yokoyama, M., Matsumoto, A. & Takeuchi, M. Solubility of uric acid and supersaturation of monosodium urate: why is uric acid so highly soluble in urine? *J. Urol.* **142,** 1095–1098 (1989).
16. Fiddis, R. W., Vlachos, N. & Calvert, P. D. Studies of urate crystallisation in relation to gout. *Ann. Rheum. Dis.* **42** (suppl. 1), 12–15 (1983).
17. Tak, H. K., Cooper, S. M. & Wilcox, W. R. Studies on the nucleation of monosodium urate at 37 °C. *Arthritis Rheum.* **23,** 574–580 (1980).
18. Loeb, J. N. The influence of temperature on the solubility of monosodium urate. *Arthritis Rheum.* **15,** 189–192 (1972).
19. Talbott, J. H. & Yu, T.-F. *Gout and Uric Acid Metabolism* (Stratton Intercontinental Medical Book Corp., New York, 1976).
20. Yagnik, D. R. *et al.* Noninflammatory phagocytosis of monosodium urate monohydrate crystals by mouse macrophages. Implications for the control of joint inflammation in gout. *Arthritis Rheum.* **43,** 1779–1789 (2000).
21. Landis, R. C. *et al.* Safe disposal of inflammatory monosodium urate monohydrate crystals by differentiated macrophages. *Arthritis Rheum.* **46,** 3026–3033 (2002).
22. Koka, R. M., Huang, E. & Lieske, J. C. Adhesion of uric acid crystals to the surface of renal epithelial cells. *Am. J. Physiol. Renal Physiol.* **278,** F989–F998 (2000).
23. Majno, G. & Joris, I. *Cells, Tissues, and Disease: Principles of General Pathology* (Blackwell Science, Cambridge, MA, 1996).
24. Bosmansky, K. & Trnavsky, K. Serum uric acid levels in disorders of the rheumatic type. *Z. Rheumatol.* **43,** 59–62 (1984).
25. Vidard, L. *et al.* Analysis of MHC class II presentation of particulate antigens of B lymphocytes. *J. Immunol.* **156,** 2809–2818 (1996).
26. Coligan, J. E., Kruisbeek, A. M., Margulies, D. H., Shevach, E. M. & Strober, W. *Current Protocols in Immunology* (Jon Wiley & Sons, Hoboken, NJ, 1991).

Supplementary Information accompanies the paper on **www.nature.com/nature**.

Acknowledgements We thank J. Sodrosky, J. Berzofsky, N. Sato, Y. Takeda and T. Vedvick for reagents; B. Zhang, P. Furcinitti and B. Kobertz for advice and technical assistance; and L. Stern and I. York for critically reviewing the manuscript. The work was supported by NIH grants to K.L.R. Y.S. was also supported by a grant from the Pittsfield TB association.

Competing interests statement The authors declare that they have no competing financial interests.

Correspondence and requests for materials should be addressed to K.L.R. (kenneth.rock@umassmed.edu).

Differential regulation of EIN3 stability by glucose and ethylene signalling in plants

Shuichi Yanagisawa[1,2], Sang-Dong Yoo[2] & Jen Sheen[2]

[1]*Research Institute for Bioresources, Okayama University, Chuo 2-20-1, Kurashiki 710-0046, Japan*
[2]*Department of Molecular Biology, Massachusetts General Hospital, Department of Genetics, Harvard Medical School, Boston, Massachusetts 02114, USA*

Glucose is a global regulator of growth and metabolism that is evolutionarily conserved from unicellular microorganisms to multicellular animals and plants[1]. In photosynthetic plants, glucose shows hormone-like activities and modulates many essential processes, including embryogenesis, germination, seedling development, vegetative growth, reproduction and senescence[2,3]. Genetic and phenotypic analyses of *Arabidopsis* mutants with glucose-insensitive (*gin*) and glucose-oversensitive (*glo*) phenotypes have identified an unexpected antagonistic interaction between glucose and the plant stress hormone ethylene. The ethylene-insensitive *etr1* and *ein2* mutants have *glo* phenotypes, whereas the constitutive ethylene signalling mutant *ctr1* is allelic to *gin4* (refs 4, 5). The precise molecular mechanisms underlying the complex signalling network that governs plant growth and development in response to nutrients and plant hormones are mostly unknown. Here we show that glucose enhances the degradation of ETHYLENE-INSENSITIVE3 (EIN3), a key transcriptional regulator in ethylene signalling[6,7], through the plant glucose sensor hexokinase[8]. Ethylene, by contrast, enhances the stability of EIN3. The *ein3* mutant has a *glo* phenotype, and overexpression of EIN3 in transgenic *Arabidopsis* decreases glucose sensitivity.

To test the hypothesis that glucose modulates ethylene signalling through the transcription factor EIN3, which acts downstream of ETR1 (ref. 9) and EIN2 (ref. 10), we tested the activity of EIN3 protein tagged with the Myc epitope in maize mesophyll proto-